Flexible Rotor System Identification and Vibration Control by Using a Magnetic Bearing

J.-S. KIM AND C.-W. LEE

ABSTRACT

Experimental modal testings are performed in order to identify the modal parameters which are essential to model building of the open loop system of the rotors. By separating the forward and backward modes in two sided frequency domain, it is shown that accurate modal parameters can be obtained, resulting in accurate modelling. It is shown that the modal testing method allows clear physical insight into the behaviors of the forward and backward modes, particularly in the case of the isotropic rotor treated in this research. A suboptimal output feedback controller is designed based on a reduced order model and is applied to a flexible rotor. The instability problem arising from the spillover effects caused by the uncontrolled high frequency modes is prevented through the constrained optimization by incorporating the spillover term into the performance index. The efficiency of the proposed identification and control method is demonstrated experimentally with a flexible rotor by using a magnetic bearing as a force actuator.

INTRODUCTION

In recent years, advanced development of magnetic bearing technology enables the active control of rotor bearing systems to be practical with relatively low cost and high reliability [1]. Magnetic bearing is considered as one of the most effective force actuators in identification and control of rotating machines, since it can deliver control force without any mechanical contact.

A few attempts have been made to develop modal testing methods for rotating machinery by using classical modal testing method [2–4] and studied the dynamic characteristics of forward and backward modes [5–7]. Recently, Lee developed a complex modal testing theory for modal parameter identification of rotating machinery [8]. In control applications, Gondhalekar et al. investigated an electromagnetic damper as applied to a transmission shaft passing through a critical speed [9]. Anton and Ulbrich performed an output feedback control using a magnetic bearing in asymmetrical rotor bearing system [10], and Salm and Schweitzer discussed spillover effects resulting from the control of a flexible rotor bearing system in output feedback [11]. However, most of the previous works essentially have not accounted for the distributed parameter nature of flexible rotors, including control and observation spillover problem [12].

Jong-Sun Kim, Department of Mechanical Engineering and Design, Hankuk Aviation University, 200–1, Hwajun-dong, Koyang-shi, Kyungki-do, 411–791, Korea
Chong-Won Lee, Department of Mechanical Engineering, Korea Advanced Institute of Science and Technology, 373–1 Kusong-dong, Yusong-ku, Taejon, 305–701, Korea

In this study, the constrained output feedback controller, which primarily emphasizes the stabilization against observation/control spillover effects through the constrained optimization, is experimentally studied based on the model which is obtained through the complex modal testings by using a magnetic bearing as a force actuator. It is also experimentally shown that complex modal testing not only allows clear physical insight into the forward and backward modes, but also enables the separation of those modes in the frequency domain so that effective modal parameter identification possible.

MODELLING AND MODAL ANALYSIS

The equations of motion and of observation for a flexible rotors can be written as [13]

$$\mathbf{M}(x)\ddot{\mathbf{q}}(x,t) + \mathbf{C}(x)\dot{\mathbf{q}}(x,t) + \mathbf{K}(x)\mathbf{q}(x,t) = \mathbf{H}(x)\mathbf{u}(t) \tag{1a}$$

$$\mathbf{y}(t) = \mathbf{G}_1(x)\mathbf{q}(x,t) + \mathbf{G}_2(x)\dot{\mathbf{q}}(x,t) \tag{1b}$$

where **M**, **C** and **K**, mainly consisting of partial differential operators and symbolic functions, represent the mass, damping and stiffness operators, respectively. Each operator is neither symmetric nor positive definite due to gyroscopic effect, internal/external damping and asymmetric bearing property. $\mathbf{G}_1$, $\mathbf{G}_2$ and **H** are the displacement sensor, velocity sensor and actuator influence operators, respectively, consisting of almost Dirac delta functions since the control devices are localized, e.g. point sensors and actuators, in practice. $\mathbf{q} = [y \;\; z]^t$ is the associated distributed displacement vector along the shaft, $\mathbf{y} = [\mathbf{q}_y^t \;\; \mathbf{q}_z^t]^t \in R^r$ the output vector, and $\mathbf{u} = [\mathbf{u}_y^t \;\; \mathbf{u}_z^t]^t \in R^m$ the input vector. The displacement **q** is subject to given initial and boundary conditions. Introducing the state $\mathbf{p} = [\dot{\mathbf{q}}^t \;\; \mathbf{q}^t]^t$, Eq.(1) can be written, in state space form, as

$$\mathbf{E}(x)\dot{\mathbf{p}}(x,t) = \mathbf{A}(x)\mathbf{p}(x,t)+\mathbf{B}(x)\mathbf{u}(t) \;\text{ and }\; \mathbf{y}(t) = \mathbf{C}(x)\mathbf{p}(x,t) \tag{2}$$

By using modal transformation $\theta(\cdot) = [<\psi_1,\cdot> \; <\psi_2,\cdot> \; <\psi_2,\cdot> \; \cdots\cdots\cdots]^t$ and the modal expansion $\mathbf{p}(x,t) = \sum_{i=1}^{\infty} \varphi_i(x)\zeta_i(t)$, a set of modal equations can be obtained as

$$\dot{\zeta}(t) = \mathbf{A}_m\zeta(t) + \mathbf{B}_m\mathbf{u}(t) \;\text{ and }\; \mathbf{y}(t) = \mathbf{C}_m\zeta(t) \tag{3}$$

where

$$\mathbf{A}_m = \theta(\mathbf{A}\Phi),\; \mathbf{B}_m = \theta(\mathbf{B}),\; \mathbf{C}_m = \mathbf{C}\Phi,\; \Phi = [\varphi_1 \;\; \varphi_2 \;\; \varphi_3 \;\cdots\cdots]$$

and $\zeta = [\zeta_1 \;\; \zeta_2 \;\; \zeta_3 \;\cdots\cdots]^t$ is the complex modal state vector. The eigenfunction φ_i and the adjoint ψ_i satisfy the biorthonormality relation

$$<\psi_i, \mathbf{E}\varphi_j> = \delta_{ij} \;\text{ and }\; <\psi_i, \mathbf{A}\varphi_j> = \lambda_i\delta_{ij} \tag{4}$$

Dividing the modal state into three classes, primary, secondary and residual modes, Eq. (3) can be rewritten, neglecting the residual modes, as

$$\dot{\zeta}_p(t) = A_p\zeta_p(t) + B_p u(t),\ \dot{\zeta}_s(t) = A_s\zeta_s(t) + B_s u(t) \tag{5a}$$

$$y(t) = C_p\zeta_p(t) + C_s\zeta_s(t) \tag{5b}$$

where the n_p–dimensional primary modal state vector ζ_p is made up of the states of significance, forming a modal subspace. The secondary modal state ζ_s consists of the modes of significance in stability but insignificance in control performance. In rotor–bearing systems, especially in overhung type rotors or rigid rotors with relatively soft bearings, the primary and secondary modes are relatively well separated so that the two–time scale assumption might be well justified. By applying the singular perturbation to the secondary modes, further model reduction can be achieved so as to give

$$\dot{\zeta}_0(t) = A_0\zeta_0(t) + B_0 u(t) \text{ and } y(t) = C_0\zeta_0(t) + D_0 u(t) \tag{6}$$

where $A_0 = A_p$, $B_0 = B_p$, $C_0 = C_p$ and $D_0 = -C_s A_s^{-1} B_s$.

Introducing the Laplace transform $Y(s)$ and $U(s)$ of the vectors $y(t)$ and $u(t)$, Eq.(5) may be transformed into

$$Y(s) = H(s)U(s) \tag{7a}$$

or

$$\begin{bmatrix} Q_y(s) \\ Q_z(s) \end{bmatrix} = \begin{bmatrix} H_{yy}(s) & H_{yz}(s) \\ H_{zy}(s) & H_{zz}(s) \end{bmatrix} \begin{bmatrix} U_y(s) \\ U_z(s) \end{bmatrix} \tag{7b}$$

where the transfer function matrix $H(s)$ is given by, from equation (5),

$$H(s) = C_p(sI - A_p)^{-1}B_p + C_s(sI - A_s)^{-1}B_s \tag{8a}$$

$$= \sum_{k=1}^{n_p} \left[\frac{\varphi_k \psi_k^*}{s - \lambda_k}\right] + \sum_{k=n_p+1}^{n_p+n_s} \left[\frac{\varphi_k \psi_k^*}{s - \lambda_k}\right] \tag{8b}$$

For isotropic systems ($H_{yy} = H_{zz}$, $H_{zy} = -H_{yz}$), by introducing the complex notation $y_c(t) = q_y(t) + jq_z(t)$ and $u_c(t) = u_y(t) + ju_z(t)$, Eq.(7) can be written as

$$Y_c(s) = H_c(s)U_c(s) \tag{9}$$

where $H_c(s) = H_{yy}(s) + jH_{zy}(s)$. Y_c and U_c are the Laplace transforms of y_c and u_c, respectively.

OUTPUT FEEDBACK CONTROLLER DESIGN

Consider an optimal dynamic compensator of the form

$$\dot{z}(t) = A_z z(t) + B_z y(t) \text{ and } u(t) = C_z z(t) + D_z y(t) \tag{10}$$

with the performance index

$$J = \int_0^\infty (\zeta_0^t Q_0 \zeta_0 + z^t Q_1 z + u^t R_0 u + \dot{z}^t R_1 \dot{z}) dt \tag{11}$$

where $z \in R^{n_z}$ is the compensator state vector, and Q_0 and Q_1 are positive semi-definite, and R_0 and R_1 are positive definite. Augmenting the state of the system with the compensator equation, one obtains

$$\dot{\hat{\zeta}}(t) = \hat{A}_c \hat{\zeta}(t) \tag{12}$$

where

$$\hat{\zeta}(t) = [\zeta_0^t(t) \;\; z^t(t)]^t, \quad \hat{A}_c = \hat{A} + \hat{B}\hat{K}\hat{C}$$

$$\hat{A} = \begin{bmatrix} A_0 & 0 \\ 0 & 0 \end{bmatrix}, \hat{B} = \begin{bmatrix} B_0 & 0 \\ 0 & I \end{bmatrix}, \hat{C} = \begin{bmatrix} C_0 & 0 \\ 0 & I \end{bmatrix}, \hat{K} = \begin{bmatrix} \hat{D}_z & \hat{C}_z \\ \hat{B}_z & \hat{A}_z \end{bmatrix}$$

$$\hat{D}_z = (I - D_z D_0)^{-1} D_z, \; \hat{C}_z = (I - D_z D_0)^{-1} C_z, \; \hat{B}_z = B_z (I - D_0 D_z)^{-1}, \; \hat{A}_z = A_z + \hat{B}_z D_0 C_z$$

It is well known that the closed loop poles approximately consist of the eigenvalues $\lambda[\hat{A}_c]$ and $\lambda[A_s + B_s D_z C_s]$ [14]. Even if Re $\lambda[\hat{A}_c] < 0$ by design and Re $\lambda[A_s] \leq 0$, it does not necessarily lead to the stability condition for the secondary modes

$$\text{Re } \lambda[A_s + B_s D_z C_s] \leq 0 \tag{13}$$

The observation and/or control spillovers are unavoidable, that is $B_s \neq 0$ and $C_s \neq 0$, since the actuators or sensors cannot be located exactly on the nodes of all secondary modes. The constrained output feedback control offers a remedy to the spillover problem by minimizing the modified performance index, using the trace identity, as

$$J_a = \text{tr}[P] + \text{tr}[F^t \aleph(\hat{K}, P)] + \text{tr}[S(A_s + B_s D_z C_s)] + \text{tr}[T\{D_z - \hat{D}_z(I + D_0 \hat{D}_z)^{-1}\}] \tag{14}$$

if initial conditions are distributed on the surface of the unit sphere, where P satisfies the matrix Riccati equation

$$(\hat{A} + \hat{B}\hat{K}\hat{C})^t P + P(\hat{A} + \hat{B}\hat{K}\hat{C}) + \hat{Q} + \hat{C}^t \hat{K}^t \hat{R} \hat{K} \hat{C} = 0 = \aleph(\hat{K}, P) \tag{15}$$

$$\hat{Q} = \begin{bmatrix} Q_0 & 0 \\ 0 & Q_1 \end{bmatrix}, \hat{R} = \begin{bmatrix} R_0 & 0 \\ 0 & R_1 \end{bmatrix}$$

and $S = \text{Diag}(s_1, s_2, \cdots\cdots, s_{n_s})$ is the positive definite weighting matrix to the spillover term. Each element of S represents the weighting for the corresponding mode and F and T are the Lagrange multiplier matrices of appropriate dimensions. The necessary conditions, using the matrix minimum principle, are obtained from [13]

$$\frac{\partial J_a}{\partial F} = \frac{\partial J_a}{\partial P} = \frac{\partial J_a}{\partial \hat{K}} = \frac{\partial J_a}{\partial T} = \frac{\partial J_a}{\partial K} = 0 \tag{16}$$

EXPERIMENT

EXPERIMENTAL SET–UP

Figure 1 shows the schematic of experimental setup. The flexible shaft, 680 mm long and 30 mm in diameter, assembled with four rigid disks is supported by two self–aligning type of radial ball bearings. The system is driven by a DC–servo motor. A magnetic bearing as a force actuator is located at the free end of the overhung rotor and it consists of four identical radial electromagnets equally spaced around a 160 mm diameter disk. A pair of eddy current type proximity probes located at 0.191 m apart from the driven end as shown in Fig. 1 measure the vertical (Y) and horizontal (Z) shaft displacement. In order to measure the control force exerted on the rotor, a three axes tool dynamometer is placed between the mount fixture and the magnetic bearing.

The controller is a hybrid system consisting of analog circuits and a digital computer. The power amplifiers and compensation networks constitute the analog components which supply the control current to the magnets and ensure the linear conversion between the control current i(t) and the generated control force f(t), i.e., $f(t) = k_i i(t)$. Current stiffness k_i is 145.5 N/A when the steady state current is 0.5 A and the total airgap is 1.5 mm. A 16–bit personal computer (IBM–PC AT) equipped with 12–bit data translation device is the main part for the digital control implementation.

MODAL PARAMETER IDENTIFICATION BY COMPLEX MODAL TESTING

The modal properties of the rotor bearing system are identified through a series of modal testings. A sequence of random Gaussian signal generated by computer is D/A converted, and transformed to current through the power amplifiers, driving the magnet and exciting the rotor system. At the same time the measured magnetic force and displacement are low–pass filtered with cut–off frequency of 400 Hz, A/D converted and then stored on the memory for further processing. The experiments are repeated at several operating speeds.

In Figs. 2 and 3, typical measured frequency response functions are plotted. When the

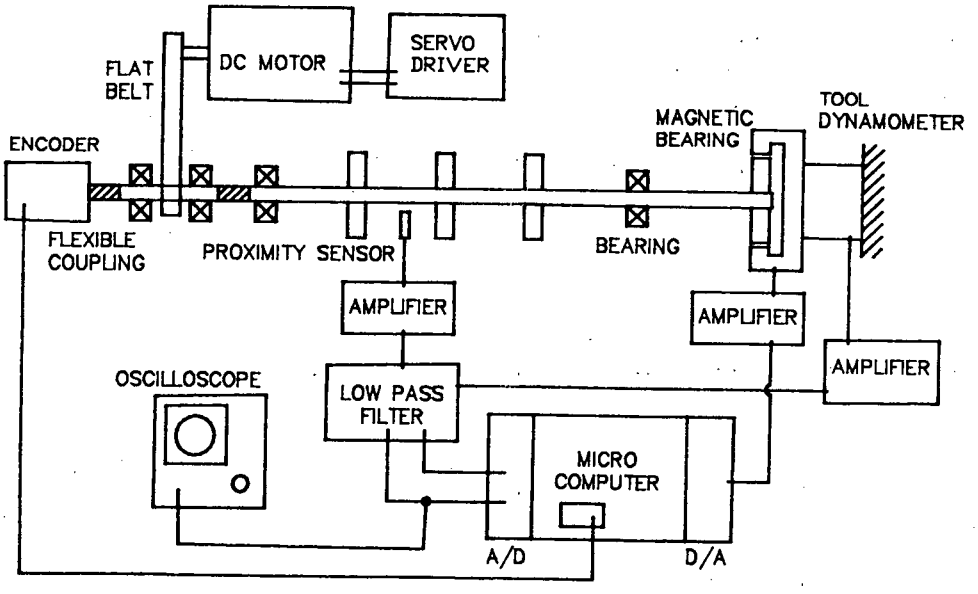

Figure 1 Schematic of experimental set–up

rotor is at rest, modal frequencies in two perpendicular directions are identical as shown in Fig.2(a), confirming that the test rig can be regarded as an isotropic system. On the other hand, the representation in the complex coordinates yields the separation of two modes into the positive and negative frequency modes in the two–sided frequency domain as shown in Fig.2(b). In this case, the use of complex notation is particularly important because it enables the accurate identification of the modal parameters as well as it reduces the computational effort by reducing dimensional size by half [8].

As the operating speed increases, the completely coupled modes become separated into the forward and backward modes since the gyroscopic moment works proportional to the rotational speed. However, those two modes are heavily overlapped in the one–sided (classical) co–quad plot, Fig.3(a). On the other hand, the forward and backward modes are completely separated in the two–sided co–quad plot, Fig.3(b), the forward on the positive frequency domain and the backward on the negative frequency domain, so that the accuracy of the modal parameter extraction is much improved.

It should be noted that, when the rotor is at rest, the transfer frequency response

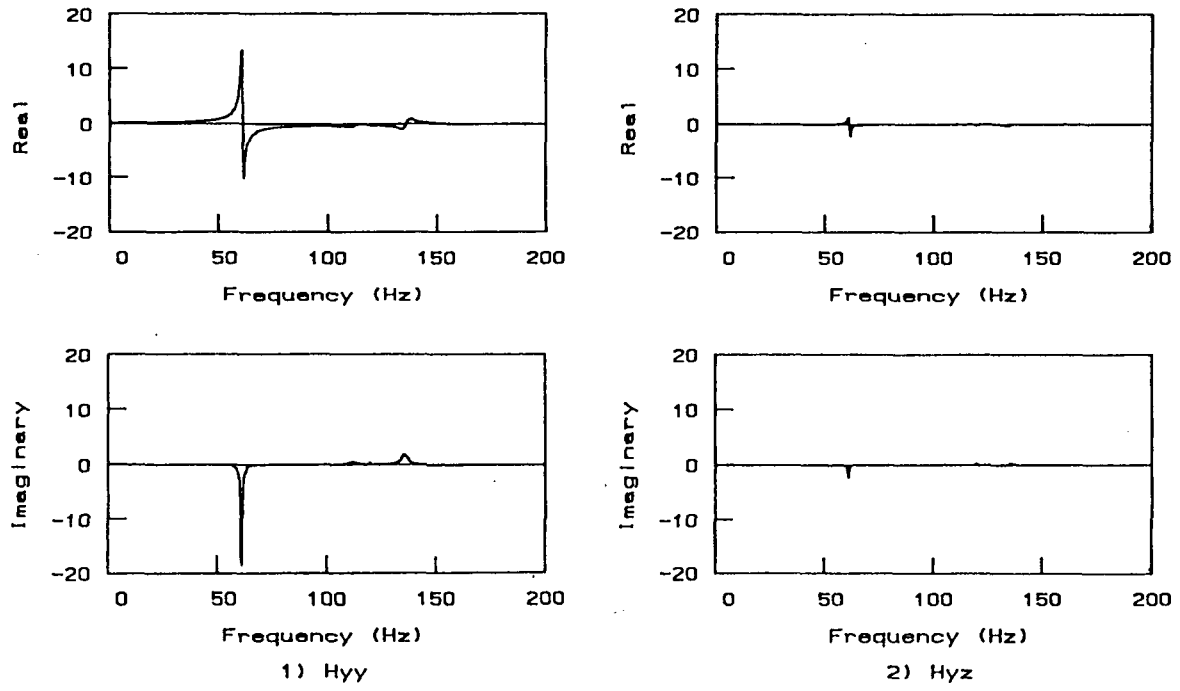

a) One–sided (classical) co–quad plots

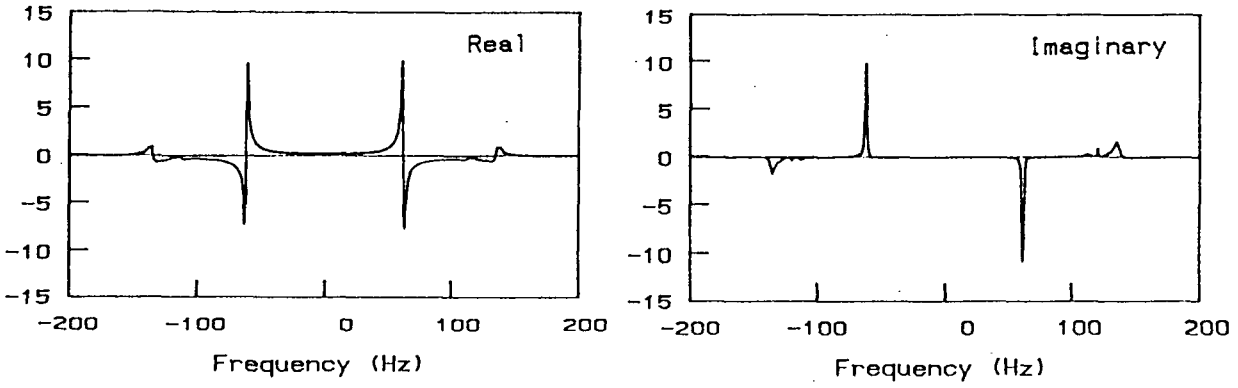

b) Two–sided co–quad plots

Figure 2 Frequency response functions (Ω = 0 rpm)

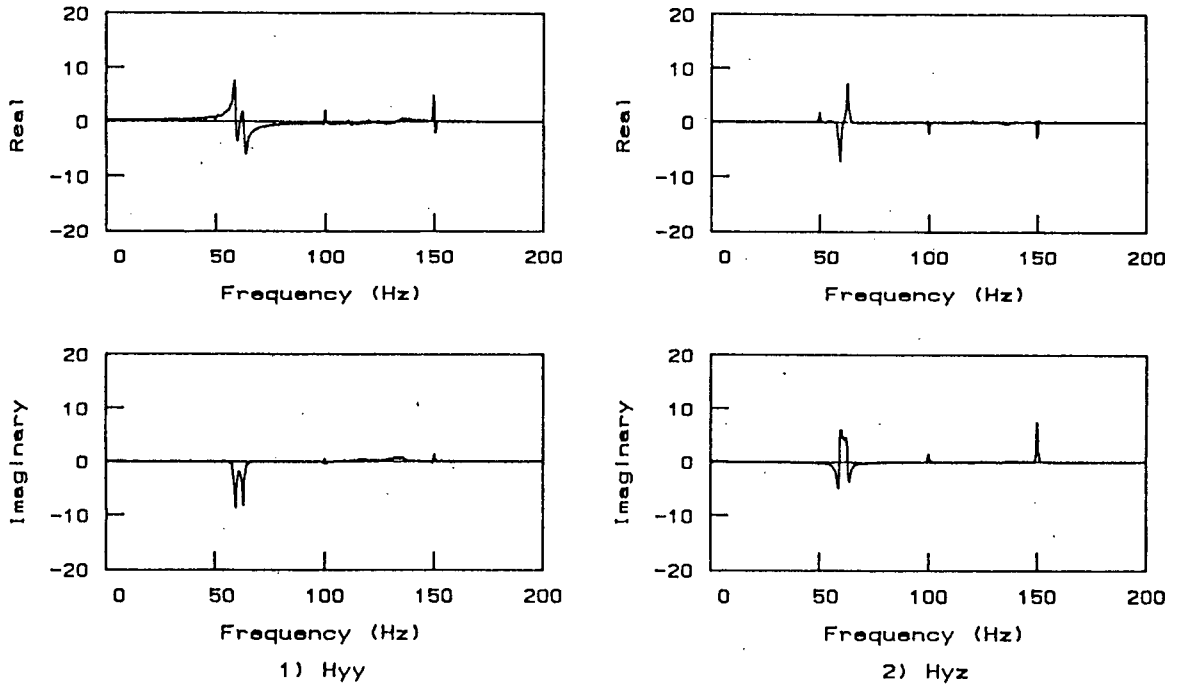

a) One–sided (classical) co–quad plots

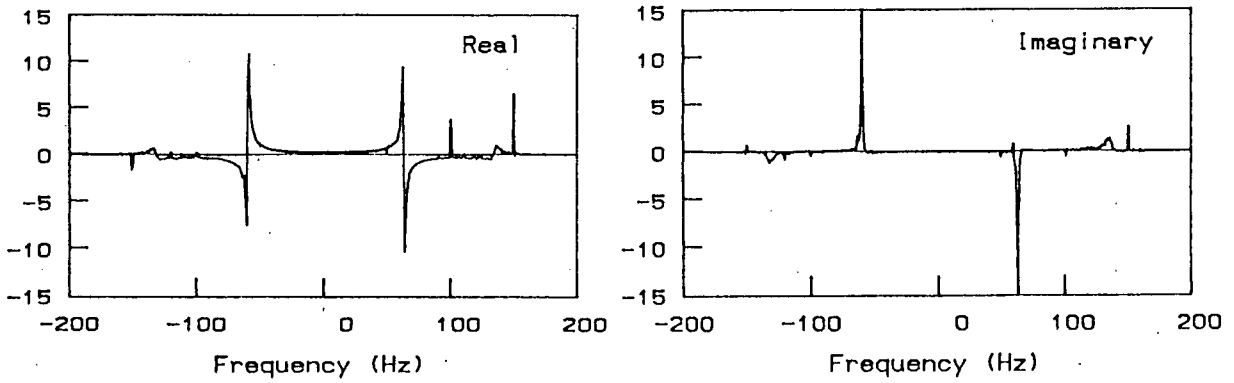

b) Two–sided co–quad plots

Figure 3 Frequency response functions (Ω = 3000 rpm)

function H_{yz} is negligibly small in magnitude compared with the direct frequency response function H_{yy} but, as the rotor starts rotating, the transfer frequency response functions are no longer negligible due to the growth of gyroscopic moments. In Table 1, the modal parameters, which are extracted by multimode curve fitting of measured frequency response functions, are summarized.

CONTROL EXPERIMENTS AND RESULTS

Using the identified modal parameters at 3000 rpm, the control model is constructed as

$$A_p=\begin{bmatrix} -3.124 & -395.495 & 0.0 & 0.0 \\ 395.495 & -3.124 & 0.0 & 0.0 \\ 0.0 & 0.0 & -3.001 & 371.808 \\ 0.0 & 0.0 & -371.808 & -3.808 \end{bmatrix}, A_s=\begin{bmatrix} -26.526 & -857.341 & 0.0 & 0.0 \\ 857.341 & -26.526 & 0.0 & 0.0 \\ 0.0 & 0.0 & -31.416 & 834.658 \\ 0.0 & 0.0 & -834.658 & -31.416 \end{bmatrix}$$

TABLE I Identified modal parameters
(F=forward mode,B=backward mode)

Rotating speed (rpm)	Mode	Natural frequency (Hz)	Damping ratio
0	1F	61.650	0.00836
	1B	61.494	0.00931
	2F	135.020	0.03470
	2B	135.030	0.03220
3000	1F	62.945	0.00790
	1B	59.175	0.00807
	2F	136.450	0.03094
	2B	132.840	0.03764

TABLE II Open loop and closed loop eigenvalues
(F=forward mode, B=backward mode)

Mode	Open loop System	Close loop System	
N		S = 0	S = 0.4I
1F	-3.124+j395.50	-33.465+j394.32	-20.468+j395.40
1B	-3.001-j371.81	-31.604-j370.78	-20.006-j371.71
2F	-26.526+j857.34	1.881+j858.91	-10.110+j857.73
2B	-31.416-j834.66	-4.304-j836.08	-15.490-j835.04

$$\mathbf{B}_p = \begin{bmatrix} 0.0 & -1.060 \\ 1.060 & 0.0 \\ 0.0 & 1.000 \\ -1.000 & 0.0 \end{bmatrix}, \quad \mathbf{B}_s = \begin{bmatrix} 0.0 & 0.520 \\ -0.520 & 0.0 \\ 0.0 & -0.497 \\ 0.497 & 0.0 \end{bmatrix}$$

$$\mathbf{C}_p = \begin{bmatrix} 0.767 & 0.0 & 0.803 & 0.0 \\ 0.0 & 0.767 & 0.0 & 0.803 \end{bmatrix} \times 10^{-4}, \quad \mathbf{C}_s = \begin{bmatrix} 0.675 & 0.0 & 0.690 & 0.0 \\ 0.0 & 0.675 & 0.0 & 0.690 \end{bmatrix} \times 10^{-4}$$

The output feedback controller is designed based on the identified modal parameters at 3000 rpm by minimizing the quadratic penalty index (14) with $\mathbf{Q}_0 = 1000\mathbf{I}$, $\mathbf{R}_0 = \mathbf{I}$, and $\mathbf{S} = s\mathbf{I}$ where the first forward and backward mode pair are chosen as the primary modes and the second mode pair as the secondary modes. As shown in Table 2, the unconstrained feedback controller ($\mathbf{S} = \mathbf{0}$) makes the closed loop system unstable since one of the secondary modes (forward mode) has negative damping. Hence it is required to make the secondary modes be stable by constrained optimization. As the parameter s increases, the second modes become stable while the primary modes become less stable. As shown in Table 2, the controller with s = 0.4 is found to be satisfactory for the dual objectives, performance and stability. To implement the controller in a digital computer, the continuous time controller is discretized by using the bilinear transformation with the 1 kHz sampling rate.

Figure 4 shows the impulse response of the flexible rotor when the rotor displacement is measured at the sensor location when the computer generated impulsive force with magnitude of 70 N and duration of 0.01 sec. is applied at the actuator position in the vertical direction. The results are compared with the simulation results obtained numerically based on the experimentally determined model. As shown in Fig.4(a), the damping ratio of the open loop system is so small (about 0.008) that the transient vibration tends to sustain for a long period of time. Figure 4(b) shows the impulse response, along with the simulation results, when the constrained output feedback control acts. The increase in damping due to control is notable. Figure 4(c) shows the impulse response when the unconstrained output feedback control acts. Notice that in the unconstrained control system the second mode becomes unstable due to the spillover effects.

The uncontrolled magnitude response due to the initial unbalance in the vicinity of the first critical speed is very large as shown in Fig.5. On the other hand, the magnitude of the controlled response is satisfactory, in particular, near the critical speed.

CONCLUSION

In this study, the complex modal testing method[5] and suboptimal vibration control method[10] are experimentally verified by using a magnetic bearing. The developed magnetic bearing is an effective non–contacting type force actuator in modal testing and control of the rotating machines during operation. By separating the forward and backward modes in two–sided frequency domain, it is shown that more accurate modal parameters can be estimated. From the experimental results, it is concluded that the proposed controller can be used effectively in suppressing the transient and steady state vibrations, while preserving stability against spillover effects.

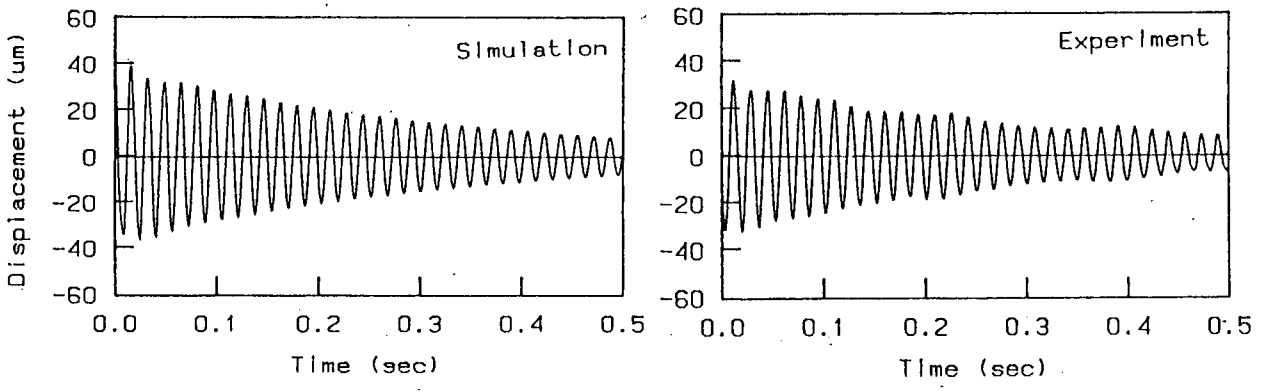

a) Open loop system

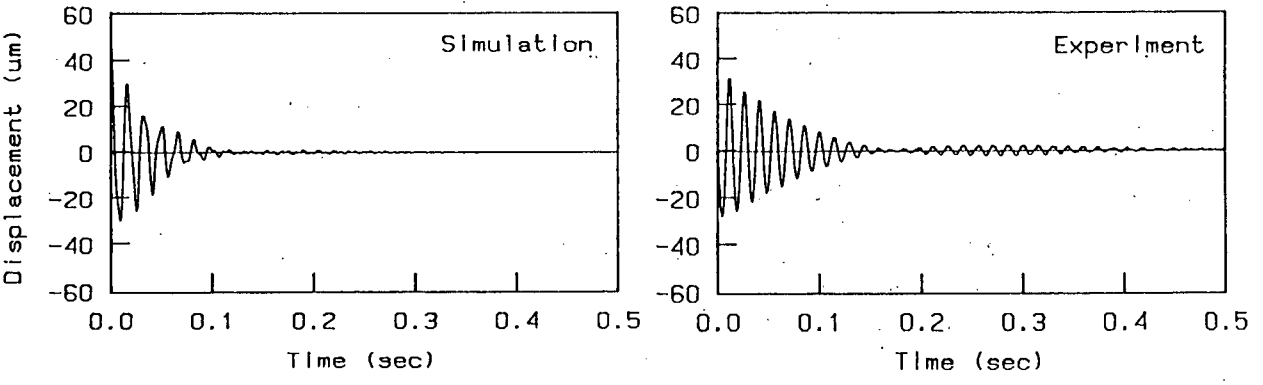

b) Constrained control; S = 0.4I

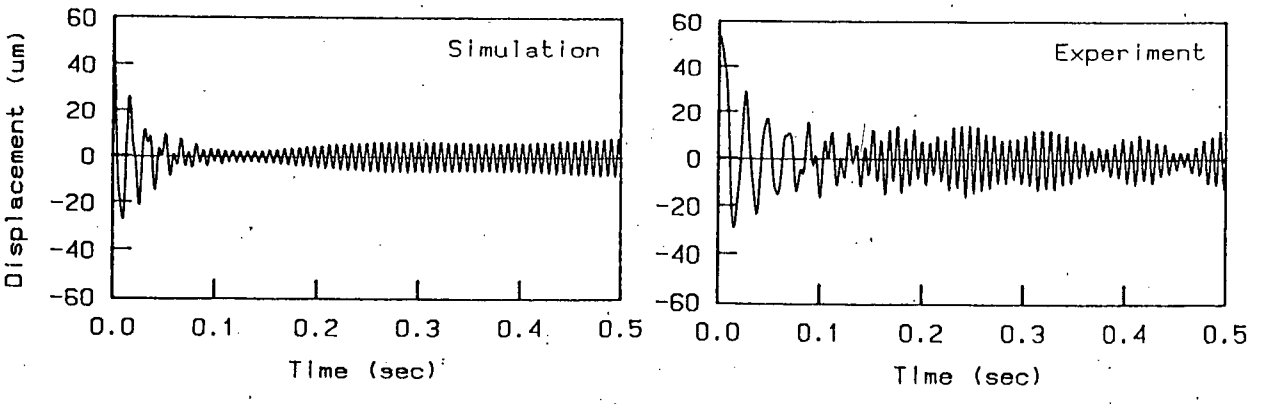

c) Unconstrained control; S = **0**

Figure 4 Transient response subject to Y–directional impulse force

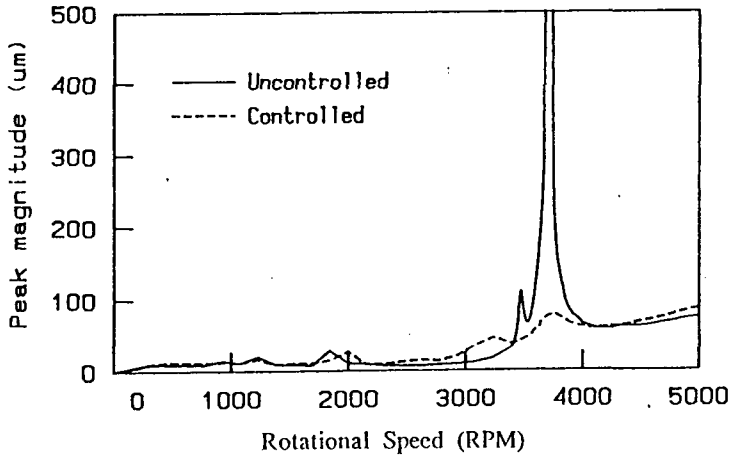

Figure 5 Unbalance response through the first critical speed

REFERENCES

1. Habermann, H., and G. Liard, 1980. "An Active Magnetic Bearing System." Tribology International, 13: 85–89.
2. Nordmann, R., 1984. "Modal Analysis in Rotor Dynamics." Dynamics of Rotors: Stability and System Identification, pp.3–21.
3. Rogers, P. J. and E. J. Ewins, 1989. "Modal Testing of an Operating Rotor System Using a Structural Dynamics Approach." Proc. of the 7th IMAC, pp.466–473.
4. Muszynska, A., 1986. "Modal Testing of Rotor/Bearing Systems." Int. J. of Analytical and Experimental Modal Analysis, 1: 15–34.
5. Matsushita, O., T. Yoshida, and N. Takahashi, 1990. "Rotor Vibration Simulation Method for Active Magnetic Bearing Control." 2nd Int. Symp. on Magnetic Bearings, pp.139–145.
6. Nonami, K. and H. Yamaguchi, 1990. "Active Vibration Control of Flexible Rotor for High Order Critical Speeds Using Magnetic Bearings." 2nd Int. Symp. on Magnetic Bearings, pp.155–160.
7. Allaire, P. E., M. E. F. Kasarda, R. R. Humphris, and D. W. Lewis, 1988. "Vibration Reduction in a Multimass Flexible Rotor Using a Midspan Magnetic Damper." 1st Int. Symp. on Magnetic Bearings, pp.149–158.
8. Lee, C. W., 1991. "A Complex Modal Testing Theory for Rotating Machinery." Mechanical Systems and Signal Processing, 5(21): 119–137.
9. Gondhalekar, V. M., J. Nikolajsen, and B. V. Jayawant, 1979. "Electromagnetic Control of Flexible Transmission Shaft Vibrations. Proc. IEE, 126: 1008–1010.
10. Anton, E., and H. Ulbrich, 1985. "Active Control of Vibrations in the Case of Asymmetrical High–Speed Rotors by Using Magnetic Bearings." ASME J. of Vibration, Acoustics, Stress, and Reliability in Design, 107: 410–415.
11. Salm, J., and G. Schweitzer, 1984. "Modeling and Control of a Flexible Rotor with Magnetic Bearings." 3rd Int. Conf. on Vibrations in Rotating Machinery, C277/84: 553–561.
12. Balas, M. J., 1978. "Active Control of Flexible Systems." J. of Optimization Theory and Applications, 25: 415–436.
13. Kim, J. S., and C. W. Lee, 1990. "Constrained Output Feedback Control of Flexible Rotor Bearing Systems." J. of Sound and Vibration, 138(1): 95–114.
14. O'Reilly, J., 1986. "Robustness of Linear Feedback Control Systems to Unmodelled High–Frequency Dynamics." Int. J. Control, 44: 1077–1088.